



RESEARCH ARTICLE

Copula-Based Modeling of Flood Control Reservoirs

10.1002/2017WR021345

M. Balistrocchi¹ , S. Orlandini² , R. Ranzi¹ , and B. Bacchi¹ 

¹Department of Civil Environmental Architectural Engineering and Mathematics, University of Brescia, Brescia, Italy,

²Department of Engineering Enzo Ferrari, University of Modena and Reggio Emilia, Modena, Italy

Key Points:

- Copulas are suitable descriptors of the statistical dependence between peak flow discharge and flood volume forcing a flood control reservoir
- The distribution of peak flow discharge released by a flood control reservoir can be obtained from the derived distribution theory
- The derived distribution of released peak flow discharge is in agreement with that obtained from time-continuous reservoir routing

Correspondence to:

M. Balistrocchi,
matteo.balistrocchi@unibs.it

Citation:

Balistrocchi, M., Orlandini, S., Ranzi, R., & Bacchi, B. (2017). Copula-based modeling of flood control reservoirs. *Water Resources Research*, 53, 9883–9900. <https://doi.org/10.1002/2017WR021345>

Received 19 JUN 2017

Accepted 19 OCT 2017

Accepted article online 24 OCT 2017

Published online 30 NOV 2017

Abstract Copulas are shown in this paper to provide an effective strategy to describe the statistical dependence between peak flow discharge and flood volume featuring hydrographs forcing a flood control reservoir. A 52 year time series of flow discharges observed in the Panaro River (Northern Italian Apennines) is used to fit an event-based bivariate distribution and to support time-continuous modeling of a flood control reservoir, located online along the river system. With regard to reservoir performances, a method aimed at estimating the bivariate return period is analytically developed, by exploiting the derived distribution theory and a simplified routing scheme. In this approach, the return period is that of the peak flow discharge released downstream from the reservoir. Therefore, in order to verify the reliability of the proposed method, a nonparametric version of its frequency distribution is assessed by means of continuous simulation statistics. Copula derived and nonparametric distributions of the downstream peak flow discharge are found to be in satisfactory agreement. Finally, a comparison of bivariate return period estimates carried out by using alternative approaches is illustrated.

1. Introduction

Flood dynamics still remains one of the most challenging research areas in applied hydrology, though it has been tackled by this discipline from its beginnings. Chief topics presently include flood prediction in ungauged watersheds (Salinas et al., 2013), estimation of climate change impact on stream flow regimes (Lehner et al., 2006), flood forecasting and uncertainty assessment (Nester et al., 2012), improvement of the direct flood frequency analysis by accounting for seasonality (Baratti et al., 2012), and mutual dependence of constituent flood variables. In particular, the latter has recently attracted increasing interest, as analysis tools of multivariate statistics have been improved by means of copula functions.

Indeed, flood control can be faced by a univariate approach relying on peak flow discharge statistics only when the main issue lies in the conveyance capacity of river cross sections. Otherwise, flood volume is the most significant variable, as in the design or safety verification of flood control reservoirs, overflow spillways, and in the flood risk mapping. Additional hydrograph shape factors, such as flood duration, time to peak, number of peaks, may have a nonnegligible influence as well.

From a theoretical point of view, implementing a multivariate distribution of a certain number of constituent variables featuring the flow discharge process represents the most effective approach in dealing with flood control. Fitting popular multivariate distribution functions (exponential (Correia, 1987), normal (Sackl & Bergmann, 1987), log-normal (Yue, 2000), and gamma (Yue, 2001)) to flood variable samples by conventional inference techniques has however proven to be neither straightforward nor completely satisfactory. As a consequence, with respect to the relevance of this topic, a relatively limited number of meaningful researches exists in literature, until recent years.

The main concern arises from having marginals belonging to the same parametric family of the joint distribution, so that transformations are used to change sample distributions accordingly. In addition to the procedure hindering and the uncertainty related to the selection of the most appropriate transformation, this expedient could result in poorer marginal fits than those achievable by different or more complex marginals.

A substantial progress has been obtained by introducing copula functions (Joe, 1997; Nelsen, 2006) in the hydrologic research field (De Michele & Salvadori, 2003; Dupuis, 2007; Favre et al., 2004; Genest & Favre,

2007). In fact, through this approach all the previously mentioned problems are effectively solved, since the dependence structure is assessed independently of marginal distributions, which can belong to different parametric families. Therefore, a large number of studies flourished in the last decade, aiming at selecting the most suitable copula functions to perform bivariate or trivariate flood frequency analyses (Chowdhary et al., 2011; De Michele et al., 2005; Ganguli & Reddy, 2013; Grimaldi & Serinaldi, 2006; Karmakar & Simonovic, 2009; Shiau et al., 2006; Zhang & Singh, 2007).

A fundamental aspect however deserves additional investigation for multivariate distribution functions to be applied in practical engineering. The estimate of multivariate return periods is actually affected by a conceptual problem all the same. The absence of a total order relation on multivariate populations makes it impossible to classify their events according to a straightforward criterion, analogous to that of univariate populations. Consequently, a criterion to split the population into the dichotomous regions of the subcritical events and the supercritical events cannot be univocally defined.

Owing to this ambiguity, several methods have been proposed up to now to provide a blanket solution to this problem, even if only a few of them truly exploit multivariate distribution potentials. Unfortunately, as can be seen in Gräler et al. (2013), such methods lead to statistically different outcomes and a generally applicable method cannot be suggested. An operative solution can however be found when facing the design, or the performance assessment, of hydraulic devices, whose failure mechanism can be related to a single variable.

Dealing with flood control dynamics by storage reservoirs, suitable hydraulic variables can be found in the maximum water stage (Requena et al., 2013) or in the maximum outflow discharge (Volpi & Fiori, 2014) occurring during the routing process. This structure oriented approach has already been followed in other practical engineering problems; for instance, Salvadori et al. (2015) and Pappadà et al. (2016) applied a multivariate technique to the design of a rubble mound breakwater, Balistrocchi and Bacchi (2017) assessed the bivariate return period of storm events defined by rainfall depth and duration, while Requena et al. (2016) faced a flood regional analysis.

Herein, the possibility of performing flood frequency analyses by categorizing bivariate event frequency with respect to the hydraulic performances of a real-world flood control reservoir is examined. An appropriate case study is given by Sant'Anna flood control reservoir (Panaro River, Padan Plain, northern Italy). A river gauge station, located in Bomporto about 10 km downstream from the reservoir, provided a 52 year long discharge series, observed before reservoir construction. A relevant practical issue has therefore arisen. In order to estimate the flooding risk in the river reach downstream from the reservoir, a direct statistical analysis will not be meaningful until the observed flow discharge series is sufficiently long, and an indirect analysis based on hydrographs entering the reservoir and related releases is needed.

A joint distribution function (JDF) of peak flow discharges and flood volumes was constructed through the copula approach, to stochastically represent the flood hydrographs forcing the reservoir. By means of a simplified hydraulic scheme based on triangular hydrographs, a routed flood frequency curve (RFFC) is finally assessed through the derived distribution theory. A numerical hydraulic model, previously described in Fiorentini and Orlandini (2013), is exploited to derive a continuous series of routed discharges. Individual event statistics of simulation outcomes is exploited to derive a benchmarking RFFC, to evaluate the reliability of the proposed probabilistic model.

Below, section 2 describes the derivation of the flood event sample from the continuous discharge series and the bivariate distribution function utilized to fit the empirical joint variability. Then, section 3 briefly recalls existing methods to estimating the return period in multivariate cases, discussing their drawbacks and limitations; afterward, the estimate method herein proposed is derived. The main hydrologic-hydraulic characteristics of the Panaro watershed and its flood control reservoir are illustrated in section 4, along with the numerical model exploited to perform continuous hydraulic simulations. Finally, the probabilistic model application is reported in section 5, where its outcomes are compared to the continuous simulation ones.

2. Peak Flow Discharge and Flood Volume Joint Distribution

In order to perform a flood frequency analysis based on copula functions, random variables uniformly distributed on the unitary interval $\mathbb{I} = [0,1]$ must be derived from the peak flow discharge q_{pi} and the flood

volume v . To do so, the probability integral transform can be exploited as shown in equation (1), where $P_{Q_{pi}}$ and P_V are the cumulative distribution functions (CDFs) of the marginal variables and r and s the corresponding uniform random variables

$$r = P_{Q_{pi}}(q_{pi}); \quad s = P_V(v) \quad \text{with} \quad (r, s) \in \mathbb{I}^2 \quad (1)$$

By using the Sklar theorem (Sklar, 1959), the JDF $P_{Q_{pi}V}$ of such flood variables can be derived according to relationship (2), where $C_\theta(r, s): \mathbb{I}^2 \rightarrow \mathbb{I}$ is the copula function that purely expresses the dependence structure

$$P_{Q_{pi}V}(q_{pi}, v) = C_\theta [P_{Q_{pi}}(q_{pi}), P_V(v)] \quad (2)$$

The most relevant issues regarding the assessment of JDF (2) can therefore be examined separately. In the following subsections, the method for identifying the independent flood events and the methods to assess the theoretical functions and their reliability are discussed.

2.1. Identification of Independent Events

Independent flood events must be isolated in the continuous discharge time series to work with random occurrences. In this regard, the partial duration series criterion has been largely applied in multivariate flood frequency analyses, since seminal papers by Todorovic were published (Todorovic, 1978). Through this criterion only those hydrographs that exceed a discharge threshold q_t are identified as individual flood events, while the remaining ones are considered low flows. This criterion is however open to criticism from two points of view.

On the one hand, it does not allow to properly distinguish the direct runoff from the base flow. Even though this aspect is essential in many hydrological applications, for instance the setup of rainfall-runoff transformation models, it is of minor concern for the design of hydraulic facilities devoted to flood control. In addition, identifying the times when direct runoff begins in the rising limb and ceases in the recession limb can be quite complex and heuristically driven, whereas the threshold strategy is straightforward and objective. With reference to flood frequency analysis, partial duration series criterion is therefore more attractive than other techniques.

On the other hand, in most practical applications, the main concern lies in extreme events, so that large q_t values are usually adopted to eliminate low return period events from the sample. This could lead to inappropriate separations of multiple peak floods. The overlapping of flood hydrographs generated by close storm events is certainly a crucial aspect. It has substantial consequences not only on the peak discharge formation, but also on flood control reservoir performances, because it affects the initial filling condition during the second event.

To prevent this, an interevent time definition IETD can be introduced (Brunner et al., 2017). As shown in Figure 1, two subsequent flood events, isolated by means of the threshold q_t criterion, are assumed to be independent only when they are separated by an interevent period greater than IETD; hence, the flow discharge below the threshold is definitely discarded. On the contrary, they are joined in a single event whose duration spans from the beginning of the former one to the end of the latter one. The independent flood event thus incorporates the flow discharge below the threshold q_t between the peaks.

In general, diverse approaches can be followed to choose suitable values for these two parameters: one focuses only on the properties of the analyzed stochastic process, another takes into consideration the hydrologic-hydraulic response of the watershed-device system. In the first one, parameter values must be such that sufficient conditions for independence are satisfied, for instance, that the annual number of occurrences suits a Poisson distribution (Todorovic, 1978). In the second one, the threshold parameter must yield hydrologic events significant to the system behavior and the performed analysis, while the minimum interevent period must be long enough for the system initial condition to be restored, when the successive event onsets (Balistocchi et al., 2013).

In consideration of its greater practical feasibility, the methodology adopted in this study follows the second approach. Hence, dealing with an online flood control reservoir, q_t and IETD were fixed so that only floods that can be appreciably attenuated by a reservoir are taken into consideration and the storage is empty at the onset of an independent flood. Once the continuous discharge series is separated into independent events, partial durations \hat{d}_j are identified. The sample of random occurrences is then derived, by

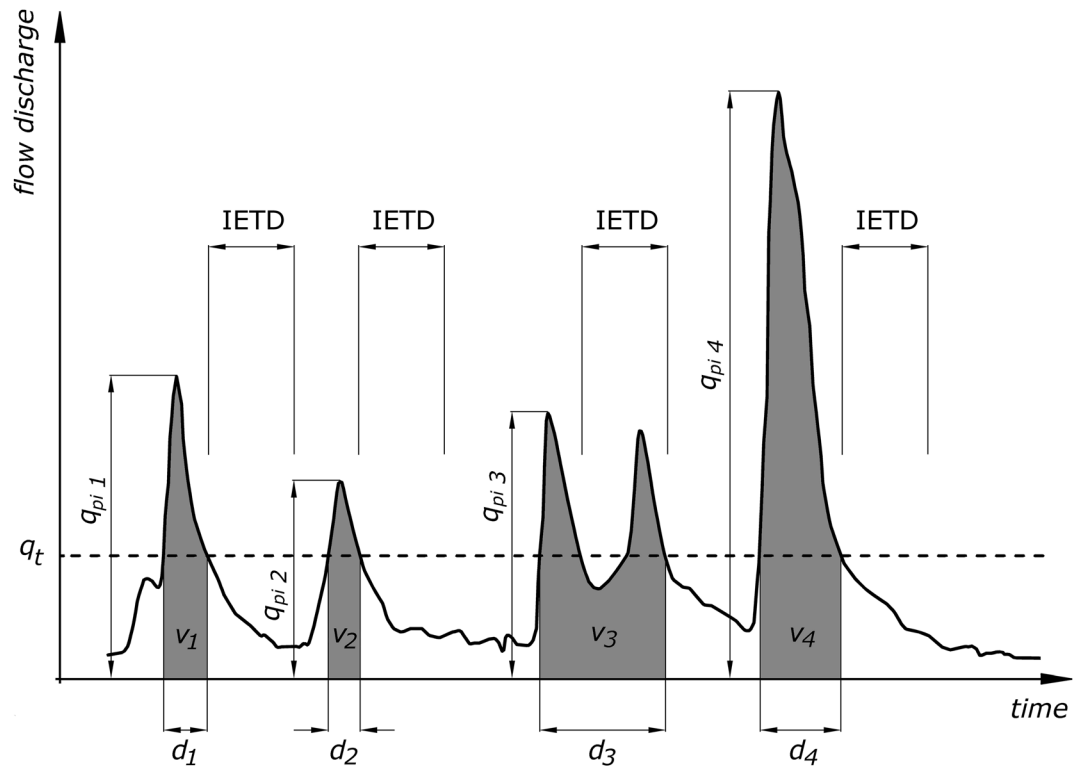


Figure 1. Example of independent event identification based on the threshold flow discharge q_t and the interevent time definition IETD, showing the relevant flood characteristics: peak flow discharges q_{pi} , flood volumes v (shaded areas), and partial durations d .

computing the peak flow discharges \hat{q}_{pij} and the flood volumes \hat{v}_j as the maximum and the integral of the total observed discharge in the partial series. An estimate of the average annual number of flood occurrences ω is obtained at the same time.

2.2. Dependence Structure Modeling

A review of the existing literature leads to the conclusion that a significant number of researches agrees on indicating the Gumbel-Hougaard copula as the most suitable choice to model the dependence structure relating to the peak flow discharge and the flood volume (De Michele et al., 2005; Karmakar & Simonovic, 2009; Li et al., 2013; Zhang & Singh, 2007). The Clayton copula was however applied in other studies (Chowdhary et al., 2011; Shiau et al., 2006), while Ganguli and Reddy (2013) proposed the t-Student copula. In order to construct trivariate distributions including the flood duration, Ben Aissia et al. (2012) suggested the Gumbel-Hougaard copula for the peak-volume pair and the Clayton copula for the volume-duration pair.

In this study, the Clayton copula was preferred to other proposals, because it had yielded more satisfactory fits to the empirical distributions than every other function, as will be shown. This choice also allowed to limit the computational burden and the parameter assessment uncertainty. Indeed, the Clayton copula belongs to the Archimedean family, so that it is a monoparametric and explicit function. Its expression is reported in equation (3), where θ represents the dependence parameter, that delineates concordant associations for $\theta > 0$, discordant associations for $\theta < 0$, and independent associations in the limiting case $\theta = 0$

$$C_\theta(r, s) = [\max\{ (r^{-\theta} + s^{-\theta} - 1), 0 \}]^{-\frac{1}{\theta}} \quad \text{with} \quad -1 \leq \theta < 0 \quad \text{or} \quad \theta > 0 \quad (3)$$

Archimedean copulas are symmetric, associative and can be constructed through a generator function $\psi : \mathbb{I} \rightarrow [0, \infty]$ as shown in relationship (4); details can be found in Salvadori et al. (2007). The Clayton copula generator function ψ is recalled in equation (5)

$$C_{\theta}(r, s) = \psi [\psi(r) + \psi(s)]^{-1} \tag{4}$$

$$\psi(t) = \frac{1}{\theta} (t^{-\theta} - 1) \quad \text{for } t \in \mathbb{I} \tag{5}$$

In a bivariate analysis, one of the greatest advantages arising from these properties is the possibility of relating θ to the Kendall rank correlation coefficient τ_k , by means of the algebraic expression (6)

$$\tau_k = \frac{\theta}{\theta + 2} \tag{6}$$

Finally, the Clayton copula features only lower tail dependence, but not upper tail dependence. Consequently, minor event dependence degree is stronger than those of other kinds of event, in particular, the extreme ones. The theoretical dependence coefficients of the lower tail λ_L and of the upper tail λ_U are reported in equation (7)

$$\lambda_L = 2^{-1/\theta}; \quad \lambda_U = 0 \tag{7}$$

In order to fit the copula function (3) to data, pseudo-observations $\{\hat{r}_j, \hat{s}_j\}$ are to be derived from the flood variable sample $\{\hat{q}_{pij}, \hat{v}_j\}$: the Weibull plotting position can be exploited as shown in equation (8), where (\hat{r}_j, \hat{s}_j) is a pseudo-observation couple, n is the sample size, and $R(\cdot)$ is the rank operator

$$(\hat{r}_j, \hat{s}_j) = \left(\frac{R(\hat{q}_{pij})}{n+1}, \frac{R(\hat{v}_j)}{n+1} \right) \quad \text{with } j=1, \dots, n \tag{8}$$

Aiming at keeping the copula fit completely apart from those of marginal distributions, two criteria can be followed: the pseudo-likelihood estimator and the moment-like method. The first one is a generally applicable method, based on the maximum likelihood criterion, while the second one can be adopted only for bivariate monoparametric copulas. In theory, the pseudo-likelihood method should lead to better fits than the moment-like method, but is much more computationally intensive. This aspect is not secondary when goodness of fit tests are performed, as they require a large number of simulation runs. In addition, in this specific application, the moment-like method gave more satisfactory fits, so that it was preferred to the first one. Therefore, copula (3) was fitted to pseudo-observations by inverting relationship (6) and substituting the sample version of the Kendall coefficient to the theoretical one.

The most objective tool to evaluate the goodness of fit achievable by means of a copula function is certainly provided by the empirical copula C_n . This is a consistent nonparametric estimator of the underlying dependence structure and can be defined, for a bivariate case, as indicated by the empirical function (9), which exploits the indicator function $\mathbf{1}(\cdot)$

$$C_n(r, s) = \frac{1}{n} \sum_{j=1}^n \mathbf{1}(\hat{r}_j \leq r, \hat{s}_j \leq s) \tag{9}$$

A preliminary evaluation of the goodness of fit can be carried out by comparing the fitted copula function to its empirical counterpart. This comparison can however give exclusively a visual understanding of the actual capability of the selected model to suit the observed dependence structure, even if can make it possible to reject the completely wrong models and to address the selection to the most suitable ones. To refine the analysis, a more objective and quantitative summary provided by tests statistics is therefore needed.

One of the most effective blanket tests is based on a rank-based version of the Cramer-Von Mises statistics (Genest et al., 2009), which accounts for the distances between the empirical copula C_n and the selected copula function, calculated in the pseudo-observations. Herein, it is defined by the sum in (10), where the copula function (3), fitted to pseudo-observations by the moment-like method, is assumed to be the underlying copula (null hypothesis)

$$S_n = \sum_{k=1}^n [C_n(\hat{r}_k, \hat{s}_k) - C_{\theta}(\hat{r}_k, \hat{s}_k)]^2 \tag{10}$$

When S_n values are low, the copula function and the empirical copula are close, on the contrary, they considerably disagree. In the latter condition, the null hypothesis is basically rejected, while, in the other, it is not. As demonstrated by Genest et al. (2009), the statistic S_n is actually able to yield an approximated p -

value, that is an empirical estimate of the probability of rejecting the null hypothesis when it is true, if it is implemented inside an appropriate parametric bootstrap procedure.

Thus, the statistics S_n (10) can be compared to those calculated with respect to simulated pseudo-observation samples, generated under the null hypothesis (Salvadori & De Michele, 2006). An approximated *p-value* is thus provided by expression (11), in which m , much larger than n , is the number of simulation runs and $S_{n,i}$ is S_n statistics corresponding to the i th simulated sample

$$p\text{-value} = \frac{1}{m} \sum_{i=1}^m \mathbf{1}(S_{n,i} > S_n) \tag{11}$$

As already underlined by Poulin et al. (2007), a great attention must be paid to detecting and, in the case, accounting for tail dependencies; on the contrary, the return period estimate would be affected by unacceptable errors. Hence, in addition to the above mentioned evaluations regarding the global goodness of fit, a more detailed analysis of the tail behaviors must be carried out. Actually, several empirical estimators of the upper tail coefficient (Frahm et al., 2005) have been developed. Unfortunately, they can only provide a term of comparison to theoretical coefficients and are strongly biased, if the upper tail dependence does not exist, or exhibits high variance (Serinaldi et al., 2015). Conversely, the lower tail dependence has attracted much less attention, since it can be assessed by means of upper tail dependence estimators applied to survival empirical copulas.

Herein, χ -plots developed by Fisher and Switzer (1985) have been preferred in spite of other tests, since they provide a more versatile tool to investigate both upper and lower tail dependencies. A χ -plot is obtained as a scatterplot of the departure from bivariate independence χ versus the distance from the bivariate median λ and, unlike other graphical tools for bivariate copula assessment, these rank-based plots clearly evidence distinctive patterns and clustering depending only on the underlying copula. To make evident the test significance, Fisher and Switzer (2001) determined χ boundary limits for statistical independence, which can be expressed as the reciprocal of the sample size square root and a parameter function of the test significance.

As underlined by Abberger (2005), this test subdivides the complete data scatter into four subsets with respect to quadrants centered in the bivariate median and it can be used to make evident tail dependences as well. When data only from the upper-right quadrant are used to construct the χ -plot, the upper tail dependence properties are depicted. The same occurs for the lower tail dependence by using data from the lower-left quadrant.

2.3. Marginal Distribution Modeling

To represent marginal variable distributions, CDFs usually employed to suiting extreme event variability were used. Satisfactory fits were then evidenced for the peak flow discharge q_{pi} by the generalized extreme value distribution (GEV) and for the flood volume v by the log-normal distribution (LN).

Equation (12) defines the peak flow discharge marginal $P_{Q_{pi}}$: κ_Q is the shape parameter, μ_Q is the location parameter, and σ_Q is the scale parameter

$$P_{Q_{pi}}(q_{pi}) = \begin{cases} \exp \left[- \left(1 + \kappa_Q \frac{q_{pi} - \mu_Q}{\sigma_Q} \right)^{-\frac{1}{\kappa_Q}} \right] & \text{for } q_{pi} > \mu_Q - \frac{\sigma_Q}{\kappa_Q} \\ 0 & \text{otherwise} \end{cases} \tag{12}$$

Equation (13) instead recalls the flood volume marginal P_V , where $\mu_{ln(v)}$ and $\sigma_{ln(v)}$ are the mean and the standard deviation of the flood volume natural logarithm and play the role of location and scale parameters

$$P_V(v) = \begin{cases} \frac{1}{\sigma_{ln(v)} \sqrt{2\pi}} \int_0^v \frac{1}{\xi} \exp \left[- \frac{1}{2} \left(\frac{\ln \xi - \mu_{ln(v)}}{\sigma_{ln(v)}} \right)^2 \right] d\xi & \text{for } v \geq 0 \\ 0 & \text{otherwise} \end{cases} \tag{13}$$

The goodness of fit of such CDFs, fitted through the maximum likelihood criterion, were verified by using the conventional confidence boundary test.

3. Return Period Estimate

There exist several approaches in literature for estimating the return period associated with multivariate events. The reason lies in the difficulty of straightforwardly generalizing its operative definition from the well-known formulation of the univariate case to the multivariate one. In equation (14), the return period T_r of a random variable x is evaluated by means of its nonexceedance probability P_X and the annual average number of occurrences ω

$$T_r(x) = \frac{1}{\omega [1 - P_X(x)]} \tag{14}$$

According to relationship (14), the random variable population is implicitly separated in two dichotomous regions: events lower than or equal to x (subcritical events) and events strictly larger than x (supercritical events). Such a self-evident criteria bases on the total order relationship featuring the univariate population, which unfortunately does not exist in a multivariate population, whose splits are consequently not univocal. Alternative approaches were therefore developed to overcome this difficulty, some still exploiting the concept of univariate return period, some actually exploiting multivariate distributions potentials.

In consideration of their popularity, however, it is worth recalling those belonging to the second group, which attempt to mimic the dichotomous splitting of univariate populations by means of intuitive logical expressions. In the so-called "OR" return period formulation, a supercritical event occurs when at least one of the random variables defining the event of interest is exceeded. Conversely, in the "AND" return period formulation, a supercritical event occurs when all the random variables are exceeded. These criteria can be easily expressed in terms of copula functions, as shown in equations (15) and (16) (Salvadori et al., 2007)

$$T_r^{OR}(r, s) = \frac{1}{\omega [1 - C_\theta(r, s)]} \tag{15}$$

$$T_r^{AND}(r, s) = \frac{1}{\omega [1 - r - s + C_\theta(r, s)]} \tag{16}$$

Although both methods actually based on a multivariate approach, they usually yield very different return period estimates, as T_r^{OR} is less equal than T_r^{AND} . The real value is arbitrarily supposed to be included in this range. In addition, they do not induce a dichotomic splitting of the population, as in the univariate case. Iso-lines of constant return period are given by copula contour lines, in the "OR" return period formulation, or survival copula contour lines in the "AND" return period one. Distinct events belonging to such lines therefore have the same return period, though their subcritical regions are different and partially overlap.

In view of these critical concerns, Salvadori and De Michele (2010) developed a method based on the Kendall function $K_C(t)$. This is a function relying only on the underlying copula that estimates the probability that an event (r, s) is included in the region bounded by the lower-left corner of the unit square and the copula contour line of level $t \in \mathbb{I}$, being $C(r, s) = t$.

The function $K_C(t)$ can be interpreted as a univariate probability distribution exclusively depending on the copula and it can be formally substituted in equation (14) to the nonexceedance probability P_X , obtaining equation (17). Since all events belonging to the contour line of level t have the same subcritical region, the Kendall function is related to a dichotomic splitting of the unitary square \mathbb{I}^2

$$T_r^{KEN}(r, s) = \frac{1}{\omega [1 - K_C(C_\theta(r, s))]} \tag{17}$$

Archimedean copulas admit an algebraic expression for the Kendall function that can be derived from the generator function ψ , as shown in equation (18), where the generator (5) of the Clayton copula is substituted

$$K_C(t) = t - \frac{\psi(t)}{\psi'(t)} = t + \frac{t}{\theta} (1 - t^\theta) \tag{18}$$

This paper has undoubtedly given a great contribution to clarifying some key aspects of the return period generalization to the multivariate framework. Nevertheless, the applicability of their proposal does not appear to be blanket. In certain real-world applications, it actually demonstrates to be affected by crucial

drawbacks and to yield unacceptable estimates, very similar to the “OR” return period formulation. For instance, Gräler et al. (2013), who investigated the exploitation of such return period estimate methods to the derivation of synthetic design flood hydrographs, found that identifying a definitively suitable method is impossible and the best solution must be selected with reference to the analysis aim.

Indeed, from an engineering point of view, facing the return period estimate by a multivariate approach makes sense only if hydraulic performances of the device of interest are significantly affected by multiple features of the hydrologic input. In this context, the severity of hydrologic events can be classified with respect to device performances. It is however important to underline that estimate methods derived by using this approach are strictly specific of the analyzed problem and cannot be generalized to other kinds of application. In addition, the return period estimate depends on the device hydraulic characteristics. Focusing on flood frequency analysis, flood control reservoir design and safety verification are typical problems in which upstream peak flow discharge and flood volume are involved.

As routing performances are usually evaluated by using downstream peak flow discharge, this variable can suitably be exploited to categorizing event severities. Therefore, all floods leading to an identical downstream peak flow discharge can be associated with the same severity, that is, the same return period. A constant value of the downstream peak flow discharge corresponds to a return period isoline in the bivariate population of input variables, which is split in two dichotomous regions: flood events belonging to the subcritical one lead to lower downstream peak flow discharges, while flood events belonging to the supercritical one lead to larger downstream peak flow discharges. In accordance with the derived distribution theory, the nonexceedance probability of the downstream peak flow discharge equals that of the bivariate flood event, allowing to trace the bivariate return period estimate back to the univariate one (Eagleson, 1972).

Nonexceedance probability of the downstream peak flow discharge can be estimated either by integrating the copula density over the delimited subcritical region, or by using conventional univariate techniques. For instance, Requena et al. (2013) utilized copula simulation techniques to generate from a bivariate distribution of peak flow discharge and flood volume a number of flood events, forcing a real-world flood control reservoir. Hydraulic simulations were then utilized to obtain maximum water stages occurring in the storage volume during the routing process. Empirical frequencies of the maximum water level were then associated to flood events.

Similarly, Volpi and Fiori (2014) faced the problem of an idealized spillway from a more theoretical point of view, by assuming a constant inflow discharge and a linear behavior for the upstream reservoir. The analytically closed-form transformation function relating the inflow peak flow discharge and the flood volume to the routed peak flow discharge was exploited to delimitate subcritical regions in the population of inflow flood variables. The bivariate return period was therefore computed with reference to nonexceedance probabilities, obtained by integrating on such regions copula density functions suggested in literature.

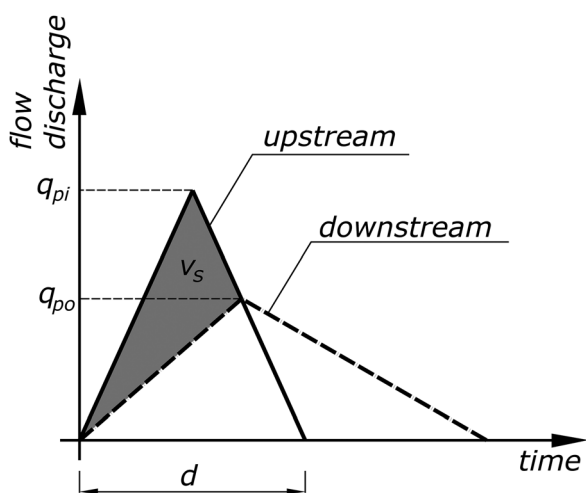


Figure 2. Simplified reservoir routing scheme highlighting the maximum stored volume v_s (grey area).

In our approach, the possibility of successfully exploiting a simplified routing scheme to represent the routing behavior of a real-world reservoir is evaluated. Actually, avoiding numerical simulations of the routing process would result in a significant decrease in the computational burden. The downstream peak flow discharge q_{po} is chosen as a dependent variable and related to the upstream peak flow discharge q_{pi} and the flood volume v through an algebraic expression. To do so, the triangular shape illustrated in Figure 2 can be given to the upstream hydrograph and the routed hydrograph. According to other studies (Balistrocchi et al., 2013; Guo & Adams, 1999; Wycoff & Singh, 1976), despite its simplicity, this scheme is actually capable to catch the main features of the routing hydraulics and permits to completely define the flood hydrograph by using two random variables. Moreover, for a given peak flow discharge-flood volume pair, this scheme basically leads to shorter flood durations than those expected in real-world floods. This should determine more rapid rising limbs and a more conservative estimate of the RFFC.

The flood duration is in fact given by ratio (19) and is accounted for as a dependent variable

$$d = \frac{2v}{q_{pi}} \tag{19}$$

The maximum volume v_s stored during the routing process amounts to the grey area in Figure 2, included between the upstream hydrograph and the downstream hydrograph, and can be easily referred to the other variables, as indicated in expression (20)

$$v_s = \frac{1}{2}d (q_{pi} - q_{po}) \tag{20}$$

Both v_s and q_{po} are random variables depending on hydrograph characteristics, so that a further relationship must be established to reduce the problem to a univariate case. Such a relationship is herein simplified in analogy with the conceptual model of the linear reservoir (21), by using a storage constant k . This linearization accounts for an average behavior of orifices and weir discharges, both operating during major flood routings

$$v_s = k q_{po} \tag{21}$$

The outflow peak flow discharge q_{po} is thus expressed only as a function of the input random variable q_{pi} and v , as shown in equation (22). This is a surjective function that allows to delimitate q_{po} isolines in the bivariate population of flood variables, which is split into two dichotomous subsets

$$q_{po}(q_{pi}, v) = \frac{v q_{pi}}{v + k q_{pi}} \tag{22}$$

By means of the derived distribution theory, such isolines can be associated with a univariate return period. The nonexceedance probability $P_{Q_{po}}$ of the downstream peak flow discharge, defined in (23), can therefore be expressed in terms of input random variables q_{pi} and v

$$P_{Q_{po}}(q_{po}) = \text{Prob}\{Q_{po} \in \mathbb{R}^+ | Q_{po} \leq q_{po}\} = \text{Prob}\left\{q_{pi}, v \in \mathbb{R}^+ \mid \frac{v q_{pi}}{v + k q_{pi}} \leq q_{po}\right\} \tag{23}$$

Inverse CDFs (1) can obviously be substituted in equation (23), for q_{po} to be expressed in terms of uniform random variables r and s , as shown in (24)

$$q_{po}(r, s) = \frac{P_V^{[-1]}(s) P_{Q_{pi}}^{[-1]}(r)}{P_V^{[-1]}(s) + k P_{Q_{pi}}^{[-1]}(r)} \tag{24}$$

The subcritical region Λ referred to a bivariate event (r, s) accounts for all events leading to a downstream peak flow discharge less than $q_{po}(r, s)$. This region is independent of the copula, conversely depends on marginals and hydraulic characteristics of the flood control reservoir, summarized by the storage constant k

$$\Lambda(r, s) = \{R, S \in \mathbb{I}^2 | q_{po}(R, S) \leq q_{po}(r, s)\} \tag{25}$$

Integrating the copula density function c_θ over this region, the nonexceedance probability of q_{po} is assessed

$$P_{Q_{po}}(r, s) = \int_{\Lambda(r, s)} c_\theta(\zeta, \phi) d\zeta d\phi \tag{26}$$

Therefore, the return period $T_r^{Q_{po}}$ featuring the bivariate event (r, s) is evaluated by means of the derived CDF (26), according to the univariate formulation (14)

$$T_r^{Q_{po}}(r, s) = \frac{1}{\omega [1 - P_{Q_{po}}(r, s)]} \tag{27}$$

4. Test Case

A test case suitable for the application of the return period estimate method herein developed was found in the Panaro River. This river is the last right-bank tributary of the Po River (northern Italy), whose geographical position is sketched in Figure 3a. The Panaro River springs from the northern edge of the

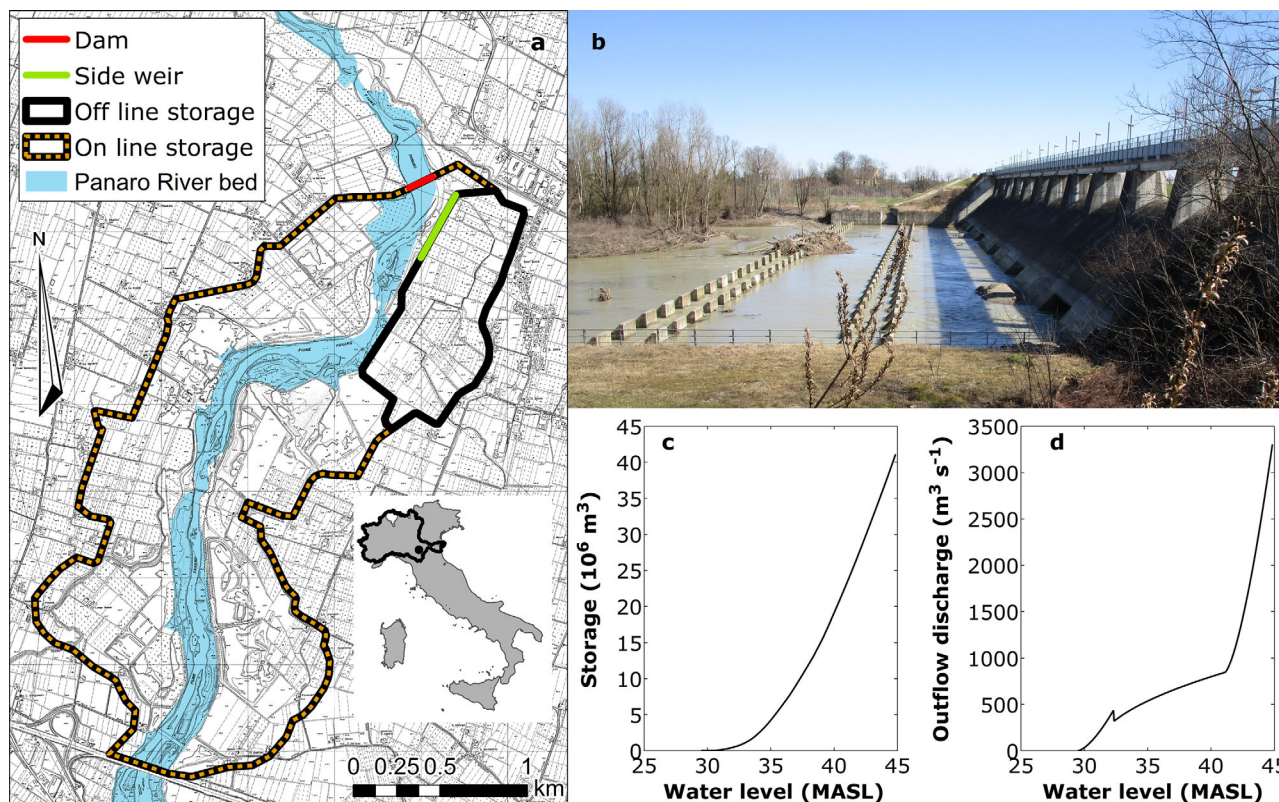


Figure 3. (a) Plan view and geographical location of Sant'Anna reservoir, (b) reservoir dam downstream side, (c) reservoir storage curve, and (d) outflow discharge curve.

Apennine chain, close to the watershed divide, and its watercourse follows an almost straight north-east direction to the outlet located in the Padan Plain. The watershed shape is quite elongated and has an almost constant width because of two relevant left-bank tributaries. Mountain catchment area is mainly natural, covered by woodland and grassland, while the plain is highly anthropized by irrigated croplands, ancient urbanizations, urban sprawls, and industrial settlements.

Flow discharge has been monitored from 1923 to 1983 by a river gauge station in Bomporto, established by the Italian hydrographic agency (Servizio Idrografico Italiano), so that data consistency amounts to 52 years. Except for a few missing observation years, this database represents an almost complete and high quality collection of hourly discharge data. This river section is located in the Padan Plain close to the junction with the Po River.

The catchment area corresponding to this river section is 1,036 km², while the main river is about 106 km long; the maximum, the average, and the minimum elevations are 2,165 MASL, 662 MASL, and 18 MASL, respectively. The time of concentration can be estimated in about 14:15 h. As can be noticed, despite the quite large catchment area, that makes the Panaro River one of the main right-bank tributaries of the Po River, the hydrologic response is relatively short.

In Bomporto river section, the discharge regime is mainly driven by the rainfall one, even if snow melt contributions can be relevant in early spring. Further, in this region, no glacier is present to sustain discharge during summer. In the Apennine side of Po River watershed, the rainfall regime is quite homogenous and is characterized by two maxima: the main one in autumn and the secondary one in spring; summer and winter are instead dry seasons. Moreover, in late spring and in summer, rainfalls are usually generated by convective storm events, featuring high intensities and short durations, but low volumes and limited spatial extensions. Conversely, in the other seasons, frontal Atlantic events bear more abundant rainfall volumes, associated with longer durations and lower intensities.

The average flow discharge is about 18 m³/s, while the maximum observed peak flow discharge is 925 m³/s and the minimum one is zero. In fact, although the mean annual rainfall depth of the Panaro watershed

(about 1,150 mm) is very close to the Italian one, conventionally assessed in 1,000 mm, dry periods may occur from July to September, when the hydrological losses increase with air temperature and the complete depletion of the snow cover in late spring are such that short duration rainfall events cannot sustain a continuous river flow.

In autumn, the discharge increasing is delayed with respect to the rainfall one, so that the most severe floods normally occur from November to December and, successively, from March to April in coincidence with the other wet season. The first period however is the most critical one since, after the fall, soil moisture is higher and canopy abstraction is minor. The short time of concentration also contributes to making such

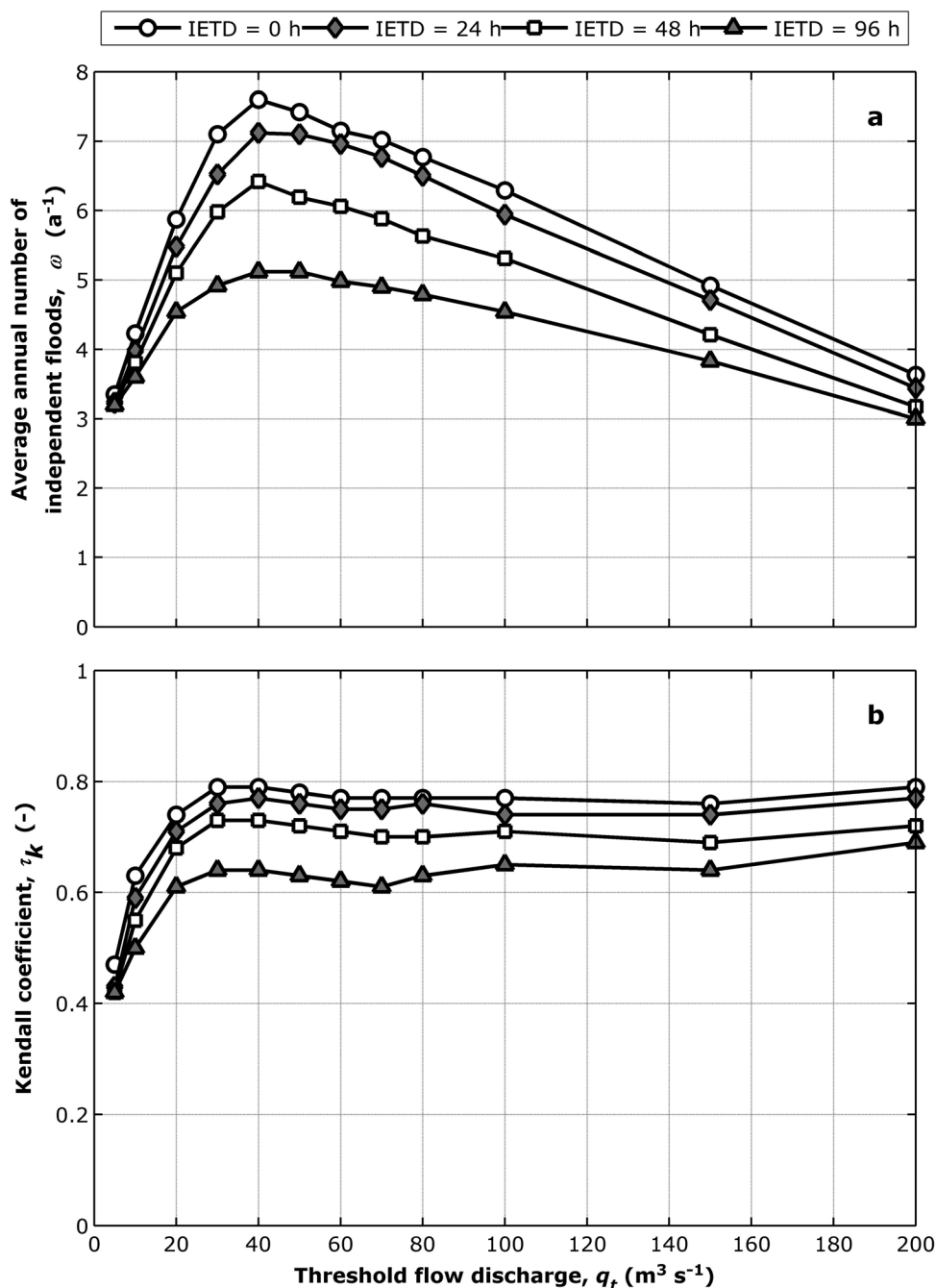


Figure 4. Trends (a) of the average annual number of independent floods ω and (b) of the Kendall coefficient τ_K with respect to the threshold flow discharge q_t and the minimum interevent time IETD.

Table 1
Sensitivity of θ , S_n , and p -Values (%) for the Clayton Copula Fitted by the Method of Moments ($m = 50,000$)

q_t (m ³ /s)	IETD (h)											
	0			24			48			96		
	θ	S_n	p -value									
5	1.75	0.030	99.6	1.51	0.033	99.1	1.47	0.033	99.0	1.44	0.033	99.1
10	3.44	0.044	94.1	2.87	0.037	97.6	2.49	0.033	99.0	2.04	0.029	99.5
20	5.73	0.038	95.9	4.93	0.032	98.6	4.19	0.030	99.1	3.12	0.032	99.0
30	7.69	0.018	99.9	6.23	0.020	99.9	5.36	0.021	99.9	3.52	0.032	99.0
40	7.50	0.018	99.9	6.53	0.018	99.9	5.53	0.023	99.8	3.50	0.040	96.0
50	7.05	0.020	99.9	6.25	0.026	99.5	5.10	0.030	98.9	3.47	0.044	94.2
60	6.55	0.020	99.9	6.05	0.023	99.8	4.86	0.030	98.9	3.30	0.048	91.9
70	6.66	0.024	99.7	6.00	0.032	98.1	4.73	0.037	96.7	3.19	0.056	86.8
80	6.84	0.024	99.7	6.18	0.030	98.6	4.63	0.035	97.5	3.35	0.044	94.0
100	6.86	0.032	98.2	5.82	0.043	93.9	4.98	0.038	96.5	3.65	0.042	94.7
150	6.36	0.064	80.0	5.72	0.061	82.3	4.52	0.053	87.9	3.55	0.058	85.0
200	7.75	0.054	86.8	6.61	0.042	93.6	5.12	0.047	91.1	4.40	0.045	92.7

flood events particularly sudden and severe. In order to reduce the hydraulic risk for the highly developed areas lying around the lower reach of the Panaro River, a flood control reservoir was built in the 1980s. The Sant’Anna flood control reservoir is located at about 8 km from the town of Modena. Latitude and longitude of the reservoir center are 44°36’00’’N and 11°00’24’’E.

Table 2
Probabilistic Model Parameters

ω (a ⁻¹)	θ (-)	κ_Q (-)	μ_Q (m ³ /s)	σ_Q (m ³ /s)	$\mu_{ln(v)}$ (-)	$\sigma_{ln(v)}$ (-)
5.3	4.98	0.27	181.40	72.86	2.80	1.01

The reservoir drains a catchment having extension of about 890 km² and is formed by a dam in concrete having a height of about 12.10 m (with respect to the base of foundations) and length of about 150 m, as shown in Figure 3b. The elevations of the reservoir bottom, the spillway crest, and the levee top are $H_B = 29.28$ m above sea level (MASL), $H_S = 40.95$ MASL, and $H_L = 44.85$ MASL, respectively. Dam supplies five rectangular bottom orifices, whose flows can be regulated by gates. As can be seen in Figure 3a, the storage capacity is mainly online, even if a minor portion (about 19%) is delimited by an inner levee. This additional offline volume is exploited only during major floods through an extended weir and emptied by a bottom orifice.

Land surface topography is known in detail by means of a 1 m digital elevation model generated from a light detection and ranging (lidar) survey carried out in 2009 by setting the point density equal to 8–10 points/m². The storage function $v_s = v_s(H)$, reported in Figure 3c, was thus determined with very high precision.

The outflow discharge function $q_o = q_o(H)$ was derived from hydraulic equations relating the head H to the outflow discharge q_o . In Figure 3d, the outflow discharge function is reported for the most common control configuration, corresponding to the all five bottom orifices completely open. As can be seen, the nonmonotonic region of the outflow discharge curve, due to the transition from the open channel flow to the pressurized pipe flow of the gated bottom orifice, is accounted for.

According to these functions, the storage volume at the maximum design elevation of 40.95 MASL is about 22.687×10^6 m³, and the outflow discharge released by the reservoir under these conditions is about 840 m³/s. As already demonstrated by Balistrocchi et al. (2013),

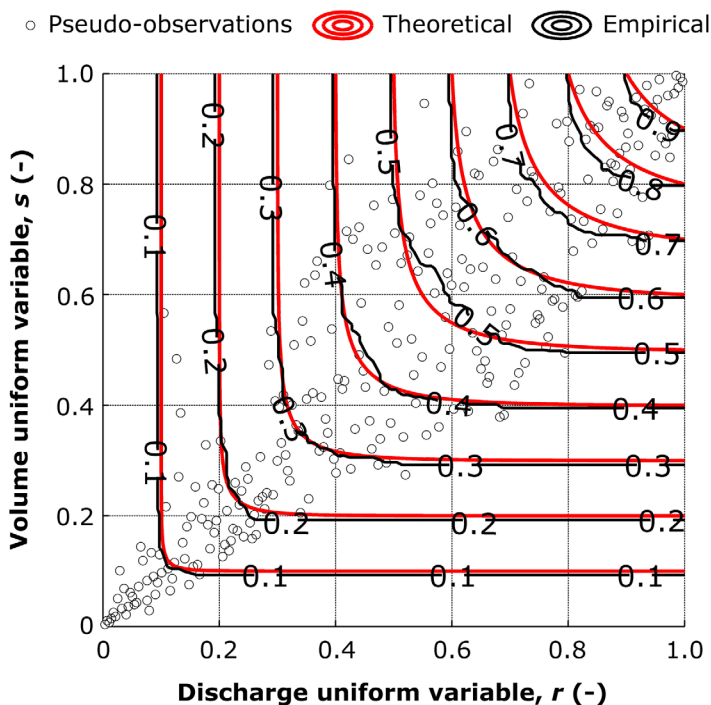


Figure 5. Visual goodness of fit evaluation of the Clayton copula to empirical copula, for selected discretization parameters, showing pseudo-observations.

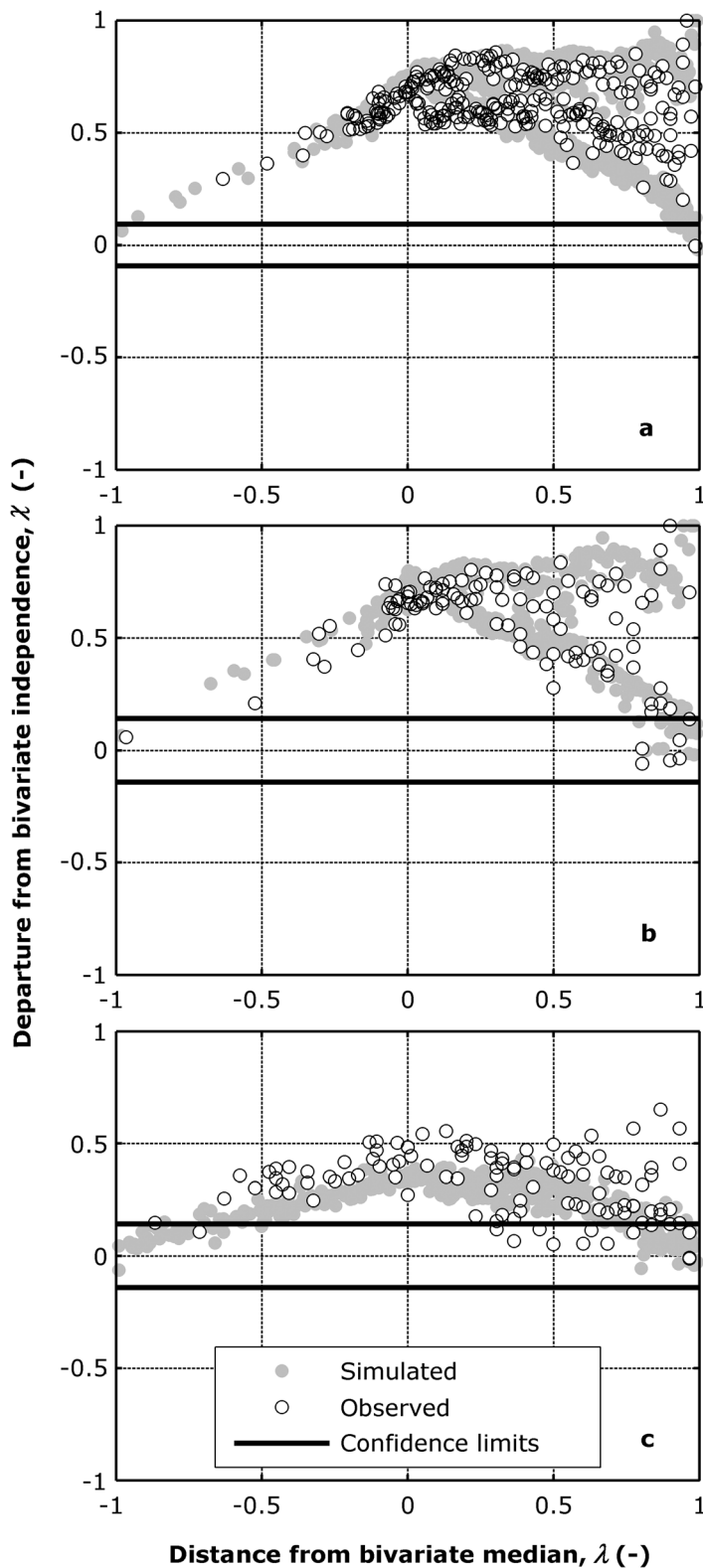


Figure 6. (a) χ^2 -plots for overall dependence, (b) lower tail dependence, and (c) upper tail dependence.

such a filling condition is suitable to assess the storage constant k by means of equation (21) that, in this case, yields a value of about 7.5 h.

The equations governing reservoir dynamics can be combined to yield the nonlinear first-order ordinary differential equation (28), where H is the water surface level, q_i is the incoming flow discharge, q_o is the total routed discharge, sum of the spillway discharge q_s and of the gated orifice discharge q_g , $A = dv_s/dH$ is the water surface area at elevation H and T is the time

$$\frac{dH}{dT} = \frac{q_i(T) - q_o(T, H)}{A(H)} \quad (28)$$

Equation (28) is normally solved numerically: practical aspects related to this problem are broadly discussed and solved as reported in Fiorentini and Orlandini (2013), where a fourth-order Runge-Kutta method, combined with a backstepping procedure controlling the time step, is suggested to obtain an accurate solution. This procedure has allowed a time-continuous simulation to be performed with no problems of model stability arising, for instance, from the nonmonotonicity of the outflow discharge curve. This last was assumed to be constant during the entire simulation period, and matching the normal control configuration of bottom orifices completely open.

5. Results and Discussion

An analysis of the probabilistic model sensitivity to the independent flood identification procedure was carried out, by varying the threshold discharge q_t and minimum interevent time IETD within quite broad ranges: 5–200 m^3/s and 0–96 h, respectively. First, the effect on the average annual number of flood events ω was computed.

As can be seen in Figure 4a, a nonmonotonic trend with respect to q_t , characterized by a quite manifest maximum, is revealed for every IETD value. This behavior appears to be reasonable in view of two contrasting occurrences when q_t rises: multiple peak floods are separated into individual independent events, while minor floods are eliminated from the event sample. When q_t is less than a few multiples of the average flow discharge, the first one prevails, conversely, when q_t increases, the second one does.

In contrast, ω systematically decreases with IETD. This is obviously expected, since the longer the IETD, the more frequent the aggregation of single-peak floods into longer multiple peak events. However, the maximum position is independent of IETD and corresponds to q_t equal to 40 m^3/s . Overall, ω spans from 7.6 to 3.0, indicating therefore a relevant sensitivity to both q_t and IETD.

In Figure 4b, instead, trends of the Kendall coefficient τ_K are plotted, showing a concordant association for every choice of q_t and IETD. Kendall coefficient τ_K increases with q_t and decreases with IETD, defining a range between 0.40 and 0.80. The association degree is however significant even for the lowest τ_K values, since the independence copula can always be rejected by test statistics (10) for p -values less than 0.1%. Moreover, τ_K increments are almost negligible when q_t is greater than 30 m^3/s . The comparison of plot a and plot b of Figure 4 allows to explain such behavior.

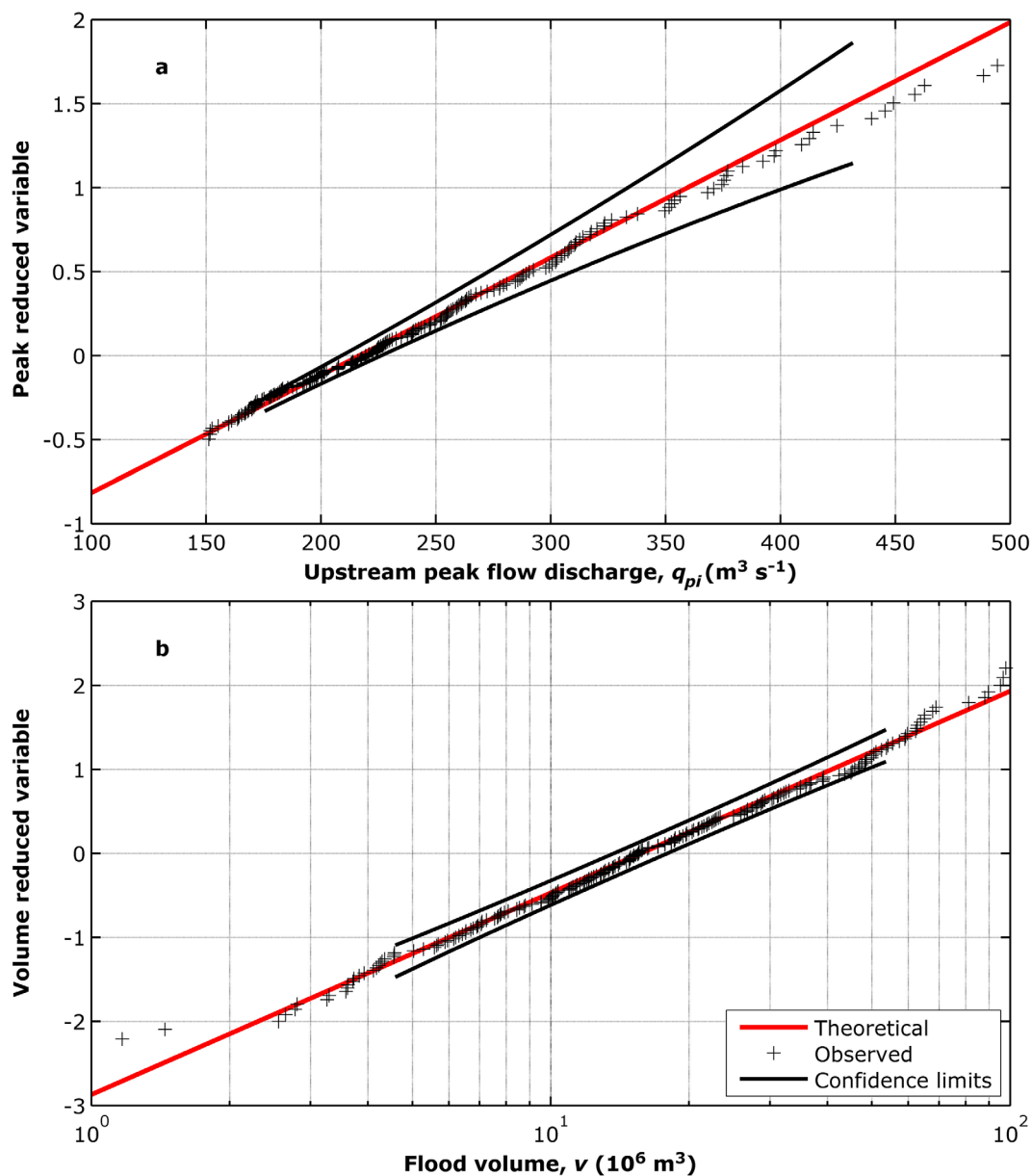


Figure 7. Confidence boundary tests (10% significance) for goodness of fit assessment of (a) peak flow discharge CDF and (b) flood volume CDF.

Concordance strengthening occurs as ω increases, that is, as multiple peak floods are progressively separated into single-peak floods. Therefore, when q_t exceeds a few multiples of the average flow discharge, floods featuring very changing hydrograph shapes are substituted by a greater number of floods having more repetitive shapes. Thus, frequencies of occurrence of flood variables tend to be more similar, increasing τ_K values. The successive suppression of minor floods does not significantly affect the achieved concordance degree. Conversely, the association weakening related to IETD lengthening is therefore due to the increase in the number of multiple peak floods.

Table 1 lists dependence parameters θ of the Clayton copula (3) along with corresponding statistics S_n (10) and p -values (11), testing the null hypothesis that the underlying copula is the Clayton copula, fitted by using the moment-like method. As the maximum sample size n is less than 300, a number of simulation runs m equal to 50,000 was considered to be sufficiently large, to obtain accurate p -value estimates. While θ obviously follows the variability of the Kendall coefficient, the goodness of fit appears to be slightly

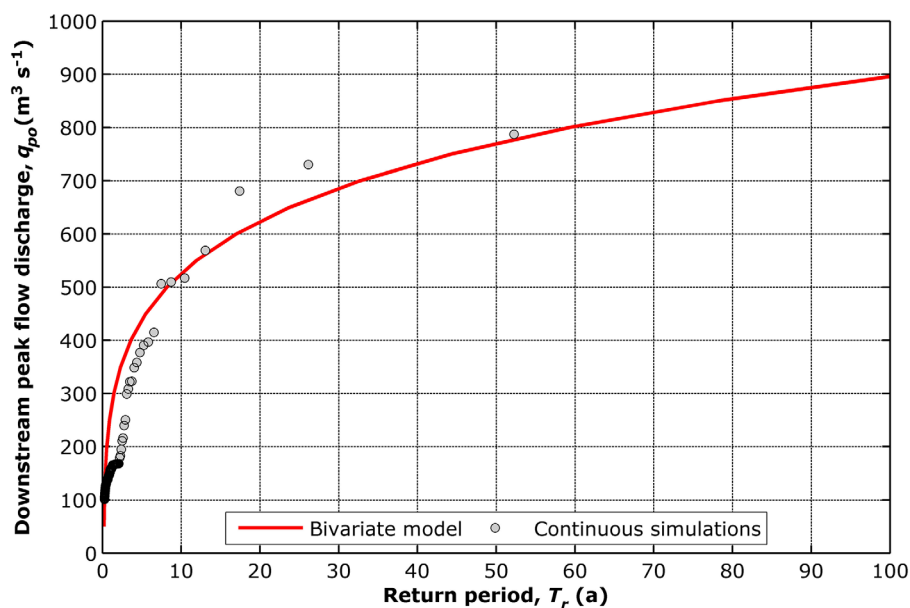


Figure 8. RFFCs derived by bivariate probabilistic approach and by continuous simulation statistics.

influenced by q_t and almost independent of IETD. In general, the null hypothesis cannot be rejected for very high p -values, the smallest one being 80.0%. This demonstrates a satisfactory capability of the Clayton copula function to fit empirical copulas. Nevertheless, a little goodness of fit detriment can be noticed when q_t exceeds the value $100 \text{ m}^3/\text{s}$.

This can only be related to the suppression of a large number of minor floods, which feature strongly associated characteristics. Since they usually have brief durations, they do not basically overlap. As previously underlined, similar hydrograph shapes tend to increase the concordance of flood variables. Thus, the resulting decreasing in the lower tail dependence strength, with respect to the overall one, may explain the detriment in the capability of the Clayton copula function to fit the empirical one.

Bearing in mind the strategy to perform the independent event identification discussed in section 2.1, suitable values of q_t and IETD were found in $100 \text{ m}^3/\text{s}$ and 48 h, respectively. Thus, IETD value is more than twice the sum of the watershed time of concentration and of the reservoir storage constant. The q_t value was instead chosen with regard to the reservoir discharge curve shown in Figure 3d and to the ω variability delineated in Figure 4a. It is evident that floods featured by a peak flow discharge less than this q_t value pass through the analyzed reservoir without any significant attenuation. Furthermore, the combination of these two parameters yields an average annual flood number of 5.3, that is considered to be, in this flow regime, a reasonable compromise both to accurately estimate low T_r (5–20 years) and to account for events significant to flood management purposes. Obtained JDF parameters are thus reported in Table 2.

A visual evaluation of the goodness of fit of the Clayton copula function to the empirical copula is illustrated in Figure 5. The satisfactory agreement that can be obtained by using this copula family, already stated by test statistics listed in Table 1, is confirmed. In particular, the lower tail dependence is modeled in a very precise manner. This is evidenced by χ -plots in Figure 6, as well. In such plots scatters of actual pseudo-observations and simulated pseudo-observations are compared (the simulated sample size n is 1,000); confidence boundaries for independence testing are reported for a significance of 10%. The overall dependence structure depicted in plot a is reported for sake of completeness, since it merely confirms the above commented outcomes.

In the regard of tail behaviors, according to this type of test, a nonnegligible lower tail dependence exists and, since actual event and simulated event scatters are in complete agreement (Figure 6, plot b), such a dependence shows to be optimally represented by a Clayton copula. The result for the upper tail dependence deserves instead some discussion: even if it appears to be sensibly weaker than the lower one, the

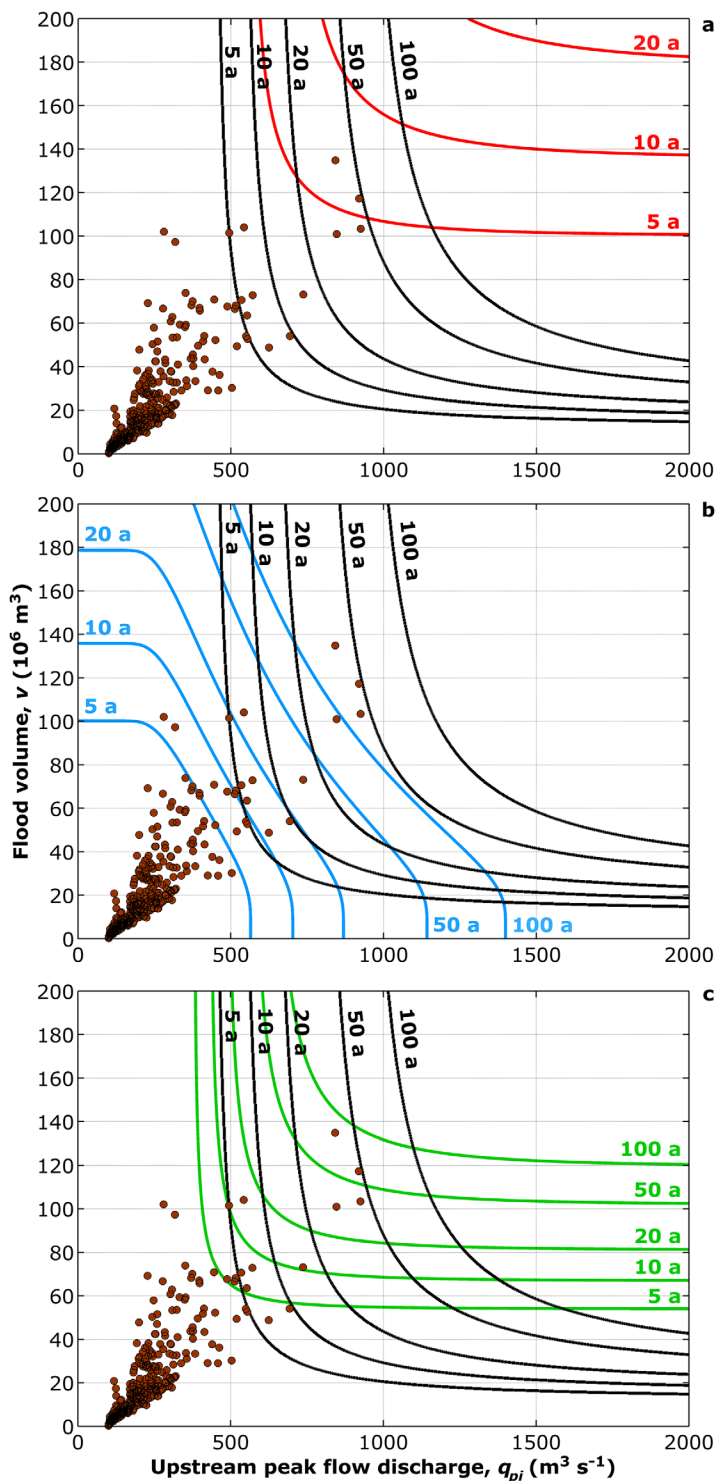


Figure 9. Comparison of return period T_r^{Qp0} isolines (black lines) to (a) T_r^{OR} isolines (red lines), (b) T_r^{AND} isolines (blue lines), (c) T_r^{KEN} isolines (green lines), and observed independent events (brown dots).

extreme events. The reason for this can be found in a better ability to mimicking routing dynamics than the others: as already underlined by some authors in different hydrologic applications (Balistrocchi & Bacchi, 2017; Serinaldi, 2015), the effectiveness of any method for splitting the multivariate population in subcritical and supercritical regions is strongly related to this crucial aspect.

independence hypothesis can be rejected for 10% significance, as most of the points are not included in the confidence region. Nevertheless, except for a few extreme events, actual event and simulated event scatters substantially agree (Figure 6, plot c), demonstrating that disregarding the upper tail dependence does not yield any appreciable goodness of fit detriment.

When other popular solutions utilized to represent peak flow discharge and flood volume association were considered, worse global fits were obtained, as larger S_n statistics were systematically assessed. More specifically, Gumbel-Hougaard copula, being an extreme value copula, better represents the upper tail but completely misinterprets the lower tail, while t-Student copula, which features identical upper and lower tail coefficients, poorly suits both tails.

Finally, marginal parameters, assessed by means of the maximum likelihood criterion, are listed in Table 2, while corresponding goodness of fit tests are reported in Figure 7, where confidence boundaries are plotted for a 10% significance. In both cases, empirical distributions completely belong to the confidence regions, so that the null hypotheses cannot be rejected.

Once the reliability of the peak flow discharge and flood volume JDF had been established, that of the routed peak flow discharge CDF was verified. Hence, the RFFC theoretically derived according to equation (27) and that obtained by statistics of the simulated routed discharge series were compared. The independent event identification in this last series was carried out by the same criterion and parameter values utilized for the incoming flow discharge. Such a comparison is shown in Figure 8, for T_r up to 100 years, evidencing a satisfactory agreement. This outcome also supports the methodology to splitting the bivariate population (25) and demonstrates the overall reliability of the approach herein developed.

Following this criterion, isolines of bivariate events (q_{pi} , v) corresponding to constant return period T_r^{Qp0} are plotted in Figure 9, where they are compared to those derived by using T_r^{OR} , T_r^{AND} , and T_r^{KEN} approaches, respectively, plots a, b, and c. In these plots, observed independent events are reported, as well. Reasonable isolines, according to which q_{pi} decreases with v , are shown for T_r^{Qp0} : to obtain an identical routed peak flow discharge, the greater the flood volume, the smaller the incoming peak flow discharge must be. It is interesting to notice that, being the analyzed 52 year series, the most severe events appropriately locate near the 50 years return period curve.

The comparison with the other return period isolines reveals that the worst result is provided by T_r^{AND} approach, as completely meaningless isolines are obtained. Differently, T_r^{OR} and T_r^{KEN} yield results more similar to those of the T_r^{Qp0} approach. However, only the second one appears to give return period values comparable to those of the T_r^{Qp0} approach, though slightly overestimated in the region of

6. Conclusions

A copula-based approach was used to derive a bivariate distribution function of two constituent flood variables, with regard to a real-world case study. This approach was found to provide an effective and straightforward strategy for inferring probability functions from multivariate sample data (Figure 5 and Table 1). Powerful tests developed inside copula framework allowed to investigate the empirical dependence structure in an accurate manner, especially with respect to the evaluation of tail dependencies (Figure 6).

Similarly to Requena et al. (2013) and to Balistrocchi and Bacchi (2017), the estimation method of multivariate return period, based on the derived distribution theory, revealed itself to be reliable. Although RFFCs were derived by using a simplified conceptual scheme, the probabilistic model yields outcomes that are in close agreement with those of more sophisticated and comprehensive continuous simulations (Figure 8). It is worth remarking that a detailed modeling of upper and lower tails plays a critical role in ensuring the overall model reliability. In fact, combining the conceptual routing scheme herein utilized with a copula featured by a relevant upper tail dependence would have led to significant underestimation of the return periods of outflow peak flow discharge.

Estimation methods previously proposed were found to give definitive mistaken contours or inaccurate estimates of the return period (Figure 9). Among them, the Kendall method (Salvadori & De Michele, 2010) however provided more realistic results than the others. This further confirms conclusions drawn by other authors (Gräler et al., 2013; Serinaldi, 2015), according to which a blanket solution to multivariate return period estimate does not exist. Conversely, the estimation method must be developed with strong reference to the practical application at hand, in order to capture the hydrologic and hydraulic mechanisms ruling the device performances.

Finally, it must be pointed out that the concept of design event, which has already undergone severe criticism in the univariate case, is meaningless in the multivariate ones. Indeed, in this bivariate flood frequency problem, there exist ∞^1 events sharing a single return period (see constant return period lines in Figure 9). In general, in a n -variate case there exist ∞^{n-1} events having constant frequency of occurrence. Therefore, from a practical point of view, the use of design event methods should be limited to preliminary device sizing, while a more reliable performance assessment should be carried out by means of continuous approaches.

In this regard, the estimation method herein proposed, which requires only a simple hydraulic parameter to be set, allows hydrologists and engineers to theoretically characterize complex river systems featuring flood control reservoirs, avoiding the computational burden of detailed numerical modeling. The need of extended flow discharge series to develop reliable JDF of flood variables nevertheless represents a problematic aspect for the application of continuous approaches, owing to the difficulty of retrieving such a kind of data.

Acknowledgments

Hydrological and hydraulic data can be downloaded upon order from <http://roberto-ranzi.unibs.it/home>.

References

- Abberger, K. (2005). A simple graphical method to explore tail-dependence in stock-return pairs. *Applied Financial Economics*, 15(1), 43–51.
- Balistrocchi, M., & Bacchi, B. (2017). Derivation of flood frequency curves through a bivariate rainfall distribution based on copula functions: Application to an urban catchment in northern Italy's climate. *Hydrology Research*, 48(3), 749–762.
- Balistrocchi, M., Grossi, G., & Bacchi, B. (2013). Deriving a practical analytical-probabilistic method to size flood routing reservoirs. *Advances in Water Resources*, 62, 37–46.
- Baratti, E., Montanari, A., Castellarin, A., Salinas, J. L., Viglione, A., & Bezzi, A. (2012). Estimating the flood frequency distribution at seasonal and annual time scales. *Hydrology and Earth System Sciences*, 16(12), 4651–4660.
- Ben Aïssia, M.-A., Chebana, F., Ouarda, T. B. M. J., Roy, L., Desrochers, G., Chartier, I., & Robichaud, É. (2012). Multivariate analysis of flood characteristics in a climate change context of the watershed of the Baskatong reservoir, Province of Québec, Canada. *Hydrological Processes*, 26(1), 130–142.
- Brunner, M. I., Viviroli, D., Sikorska, A. E., Vannier, O., Favre, A.-C., & Seibert, J. (2017). Flood type specific construction of synthetic design hydrographs. *Water Resources Research*, 53, 1390–1406. <https://doi.org/10.1002/2016WR019535>
- Chowdhary, H., Escobar, L. A., & Singh, V. P. (2011). Identification of suitable copulas for bivariate frequency analysis of flood peak and flood volume data. *Hydrology Research*, 42(2–3), 193–216.
- Correia, F. N. (1987). Multivariate partial duration series in flood risk analysis. In V. P. Singh (Ed.), *Hydrologic frequency modelling* (pp. 541–554). Dordrecht, The Netherlands: Springer.
- De Michele, C., & Salvadori, G. (2003). A generalized Pareto intensity-duration model of storm rainfall exploiting 2-copulas. *Journal of Geophysical Research*, 108(D2), 4067. <https://doi.org/10.1029/2002JD002534>
- De Michele, C., Salvadori, G., Canossi, M., Petaccia, A., & Rosso, R. (2005). Bivariate statistical approach to check adequacy of dam spillway. *Journal of Hydrologic Engineering*, 10(1), 50–57.

- Dupuis, D. J. (2007). Using copulas in hydrology: Benefits, cautions, and issues. *Journal of Hydrologic Engineering*, 12(4), 381–393.
- Eagleson, P. S. (1972). Dynamics of flood frequency. *Water Resources Research*, 8(4), 878–898.
- Favre, A.-C., El Adlouni, S., Perreault, L., Thiémond, N., & Bobée, B. (2004). Multivariate hydrological frequency analysis using copulas. *Water Resources Research*, 40, W01101. <https://doi.org/10.1029/2003WR002456>
- Fiorentini, M., & Orlandini, S. (2013). Robust numerical solution of the reservoir routing equation. *Advances in Water Resources*, 59(9), 123–132. <https://doi.org/10.1016/j.advwatres.2013.05.013>
- Fisher, N. I., & Switzer, P. (1985). Chi-plots for assessing dependence. *Biometrika*, 72(2), 253–265.
- Fisher, N. I., & Switzer, P. (2001). Graphical assessment of dependence: Is a picture worth 100 tests? *American Statistician*, 55(3), 233–239.
- Frahm, G., Junker, M., & Schmidt, R. (2005). Estimating the tail-dependence coefficient: Properties and pitfalls. *Insurance: Mathematics and Economics*, 37(1), 80–100.
- Ganguli, P., & Reddy, M. J. (2013). Probabilistic assessment of flood risk using trivariate copulas. *Theoretical and Applied Climatology*, 111(1–2), 341–360.
- Genest, C., & Favre, A.-C. (2007). Everything you always wanted to know about copula modelling but were afraid to ask. *Journal of Hydrologic Engineering*, 12(4), 347–368.
- Genest, C., Rémillard, B., & Beaudoin, D. (2009). Goodness-of-fit tests for copulas: A review and a power study. *Insurance: Mathematics and Economics*, 44(2), 199–213.
- Gräler, B., Van Den Berg, M. J., Vandenberghe, S., Petroselli, A., Grimaldi, S., De Baets, B., & Verhoest, N. E. C. (2013). Multivariate return periods in hydrology: A critical and practical review focusing on synthetic design hydrograph estimation. *Hydrology and Earth System Sciences*, 17(4), 1281–1296.
- Grimaldi, S., & Serinaldi, F. (2006). Asymmetric copula in multivariate flood frequency analysis. *Advances in Water Resources*, 29, 1155–1167.
- Guo, Y., & Adams, B. J. (1999). An analytical probabilistic approach to sizing flood control detention facilities. *Water Resources Research*, 35(8), 2457–2468.
- Joe, H. (1997). *Multivariate models and dependence concepts*. London, UK: Chapman and Hall.
- Karmakar, S., & Simonovic, S. P. (2009). Bivariate flood frequency analysis part 2: A copula-based approach with mixed marginal distributions. *Journal of Flood Risk Management*, 2(1), 32–44.
- Lehner, B., Döll, P., Alcamo, J., Henrichs, T., & Kaspar, F. (2006). Estimating the impact of global change on flood and drought risks in Europe: A continental, integrated analysis. *Climatic Change*, 75(3), 273–299.
- Li, T., Guo, S., Chen, L., & Guo, J. (2013). Bivariate flood frequency analysis with historical information based on copula. *Journal of Hydrologic Engineering*, 18(8), 1018–1030.
- Nelsen, R. B. (2006). *An introduction to copulas* (2nd ed.). New York, NY: Springer.
- Nester, T., Komma, J., Viglione, A., & Blöschl, G. (2012). Flood forecast errors and ensemble spread: A case study. *Water Resources Research*, 48, W10502. <https://doi.org/10.1029/2011WR011649>
- Pappadà, R., Perrone, E., Durante, F., & Salvadori, G. (2016). Spin-off extreme value and Archimedean copulas for estimating the bivariate structural risk. *Stochastic Environmental Research and Risk Assessment*, 30(1), 327–342.
- Poulin, A., Huard, D., Favre, A.-C., & Pugin, S. (2007). Importance of tail dependence in bivariate frequency analysis. *Journal of Hydrologic Engineering*, 12(4), 394–403.
- Requena, A. I., Chebana, F., & Mediero, L. (2016). A complete procedure for multivariate index-flood model application. *Journal of Hydrology*, 535, 559–580.
- Requena, A. I., Mediero, L., & Garrote, L. (2013). A bivariate return period based on copulas for hydrologic dam design: Accounting for reservoir routing in risk estimation. *Hydrology and Earth System Sciences*, 17(8), 3023–3038.
- Sackl, B., & Bergmann, H. (1987). A bivariate flood model and its applications. In V. P. Singh (Ed.), *Hydrologic frequency modelling* (pp. 571–582). Dordrecht, The Netherlands: Reidel.
- Salinas, J. L., Laaha, G., Rogger, M., Parajka, J., Viglione, A., Sivapalan, M., & Blöschl, G. (2013). Comparative assessment of prediction in ungauged basins—Part 2: Flood and low flow studies. *Hydrology and Earth System Sciences*, 17(7), 2637–2652.
- Salvadori, G., & De Michele, C. (2006). Statistical characterization of temporal structure of storms. *Advances in Water Resources*, 29(6), 827–842.
- Salvadori, G., & De Michele, C. (2010). Multivariate multiparameter extreme value models and return period: A copula approach. *Water Resources Research*, 46, W10501. <https://doi.org/10.1029/2009WR009040>
- Salvadori, G., Durante, F., Tomasicchio, G. R., & D'Alessandro, F. (2015). Practical guidelines for the multivariate assessment of the structural risk in coastal and off-shore engineering. *Coastal Engineering*, 95(6), 77–83.
- Salvadori, G., De Michele, C., Kottegoda, N. T., & Rosso, R. (2007). *Extremes in nature: An approach using copulas*. Dordrecht, The Netherlands: Springer.
- Serinaldi, F. (2015). Dismissing return periods! *Stochastic Environmental Research and Risk Assessment*, 29(4), 1179–1189.
- Serinaldi, F., Bárdossy, A., Kilsby, C. G. (2015). Upper tail dependence in rainfall extremes: would we know it if we saw it? *Stochastic Environmental Research and Risk Assessment*, 29(4), 1211–1233.
- Shiau, J. T., Wang, H. Y., & Tsai, C. T. (2006). Bivariate frequency analysis of floods using copulas. *Journal of the American Water Resources Association*, 42(6), 1549–1564.
- Sklar, A. (1959). Fonctions de répartition à n dimensions et leurs marges. *Publications de l'Institut de statistique de l'Université de Paris*, 8, 229–231.
- Todorovic, P. (1978). Stochastic models of floods. *Water Resources Research*, 14(2), 345–356.
- Volpi, E., & Fiori, A. (2014). Hydraulic structures subject to bivariate hydrological loads: Return period, design, and risk assessment. *Water Resources Research*, 50, 885–897. <https://doi.org/10.1002/2013WR014214>
- Wycoff, R. L., & Singh, U. P. (1976). Preliminary hydrologic design of small flood detention reservoirs. *Water Resources Bulletin*, 12(2), 337–349.
- Yue, S. (2000). The bivariate lognormal distribution to model a multivariate flood episode. *Hydrological Processes*, 14(14), 2575–2588.
- Yue, S. (2001). A bivariate gamma distribution for use in multivariate flood frequency analysis. *Hydrological Processes*, 15(6), 1033–1045.
- Zhang, L., & Singh, V. P. (2007). Trivariate flood frequency analysis using the Gumbel-Hougaard copula. *Journal of Hydrologic Engineering*, 12(4), 431–439.